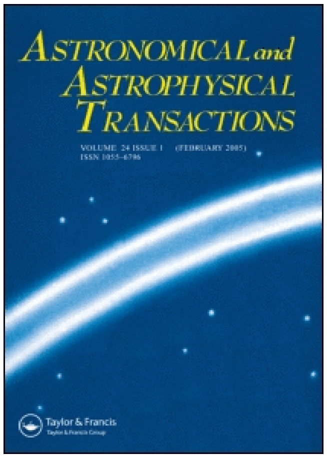

Astronomical & Astrophysical Transactions
The Journal of the Eurasian Astronomical Society
Publication details, including instructions for authors and subscription information:
http://www.informaworld.com/smpp/title~content=t713453505

Time series analysis of unequally spaced data: Intercomparison between the Schuster periodogram and the LS-spectra

V. V. Vityazev [a]
[a] Astronomy Department, St. Petersburg University, St. Petersburg, Russia

Online Publication Date: 01 November 1996
To cite this Article: Vityazev, V. V. (1996) 'Time series analysis of unequally spaced data: Intercomparison between the Schuster periodogram and the LS-spectra', Astronomical & Astrophysical Transactions, 11:2, 139 - 158
To link to this article: DOI: 10.1080/10556799608205461
URL: http://dx.doi.org/10.1080/10556799608205461

Astronomical and Astrophysical Transactions, 1996, Vol. 11, pp. 139–158
Reprints available directly from the publisher
Photocopying permitted by license only

TIME SERIES ANALYSIS OF UNEQUALLY SPACED DATA: INTERCOMPARISON BETWEEN THE SCHUSTER PERIODOGRAM AND THE LS-SPECTRA

V. V. VITYAZEV

Astronomy Department, St. Petersburg University, Bibliotechnaya, pl. 2, Petrodvorets, St. Petersburg, 198904, Russia

(Received November 9, 1995)

At present, the Schuster periodogram and the LS-spectra are widely used for evaluating the power spectra of irregularly spaced time series. According to many authorities, the LS-spectra are preferable over the Schuster periodogram since they are based on the least-squares fitting of a sine function to the data and since they have the exponential distribution when the time series is pure noise. On the other hand, the practice of spectral analysis shows that the Schuster periodogram and the LS-spectra often are almost identical. In this paper the theoretical study of all the estimators is made with the purpose to describe the situations when the Schuster periodogram differs from the LS-spestra sufficiently. It is shown that the likeness of the periodograms under consideration depends on the properties of the spectral window $W(\omega)$ corresponding to the distribution of time points. The main results are: a) all the estimators evaluated at frequency ω are identical if $W(2\omega) = 0$; b) the Schuster periodogram differs from the LS-spectra at the frequency $\omega = \bar{\omega}/2$, where $\bar{\omega}$ is the frequency at which the spectral window has a large side peak due to irregular distribution of time points. The numerical examples for several situations typical in astronomy illustrate these conclusions.

KEY WORDS Power spectra, time series

1 INTRODUCTION

In various branches of astronomy, we face the problem of finding unknown periodicities hidden in the observational data. If data are regularly spaced in time, the Discrete Fourier Transform (DFT) and the Schuster periodogram associated with it (Schuster, 1898) are the basic tools for evaluating the power spectra (Jenkins and Watts, 1968; Otnes and Enocson, 1978; Marple, 1987; Terebizh, 1992, etc.). Unfortunatly, the astronomical observations are irregular due to different reasons: day-time changes, weather conditions, positions of the object under observations and so on. The present day theory and practice of the spectral analysis of the unequally spaced time series are based on two approaches. The first one employs the Schuster periodogram for unequally spaced data (Deeming, 1975a, 1975b; Roberts *et al.*, 1987). The second one uses the procedure of the least-squares fitting of a sinusoid to the data (Barning, 1962; Lomb, 1976; Ferraz-Mello, 1981, Scargle, 1982, 1989). The resulting estimators (the so-called LS-spectra) and the modified discrete Fourier transforms associated with them are widely used nowadays. The most valuable feature of the LS-spectra is their well-defined statistical behavior. At the same time, the LS-spectra lose several very important properties: they cannot be discribed in terms of the spectral window, they cannot be strictly connected with the correlation function, etc. On the other hand, the Schuster periodogram of a gapped time series satisfies all the fundamental relations of the classical spectral analysis, but its statistical properties are complicated as compared to the case of regular data. It is worth mentioning that, despite different theoretical foundations, the Schuster periodogram and the LS-spectra frequently turn out to be almost identical. This similarity requires an explanation, and this is the main point of the present paper in which we are trying to find situations when the Schuster periodogram and the LS-spectra are very close to each other or differ greatly. The final goal of this study is to clarify the properties of various techniques which are used to derive the periodicities in the unequally distributed data.

2 THE LEAST-SQUARES PROCEDURE AS AN ESTIMATOR OF THE POWER SPECTRUM

We begin by exposing the general least-squares approach that produces various kinds of the LS-spectra. Given a set of N observations

$$x_k = x(t_k),\ k = 0, 1, \ldots, N-1$$

with zero mean obtained at arbitrary times t_k, we can set up the model

$$f(t) = \sum_{i=1}^{2} a_i \phi_i(t), \tag{2.1}$$

where

$$\phi_1(t) = \cos \omega t, \tag{2.2}$$

$$\phi_2(t) = \sin \omega t. \tag{2.3}$$

Defining the residuals of approximation as

$$\epsilon_k = x_k - f(t_k), \tag{2.4}$$

we can find the coefficients a_1 and a_2 from the condition

$$||\epsilon||^2 = \min, \tag{2.5}$$

where the following notation is used:

$$(p,q) = \frac{1}{N}\sum_{k=0}^{N-1} p(t_k)q(t_k), \tag{2.6}$$

$$||p||^2 = (p,p). \tag{2.7}$$

In our case the coefficients a_1 and a_2 are determined as the solution of the corresponding *normal equations*:

$$\begin{bmatrix} a_1 \\ a_2 \end{bmatrix} = \frac{1}{\Delta}\begin{bmatrix} ||\phi_2||^2 & -(\phi_1,\phi_2) \\ -(\phi_2,\phi_1) & ||\phi_1||^2 \end{bmatrix}\begin{bmatrix} (x,\phi_1) \\ (x,\phi_2) \end{bmatrix}, \tag{2.8}$$

where

$$\Delta = ||\phi_1||^2||\phi||^2 - (\phi_1,\phi_2). \tag{2.9}$$

Now, for the quantity

$$E_{\text{min}} = ||\epsilon||^2 = \min \tag{2.10}$$

one has

$$E_{\text{min}} = ||x||^2 - \sum_{i=1}^{2} a_i(x,\phi_i). \tag{2.11}$$

If the functions ϕ_1 and ϕ_2 are orthogonal, then

$$E_{\text{min}} = ||x||^2 - \sum_{i=1}^{2} a_i^2||\phi_i||^2. \tag{2.12}$$

Consider now the function

$$P(\omega) = ||x||^2 - E_{\text{min}} \geq 0. \tag{2.13}$$

Obviously, the function $P(\omega)$, when plotted against ω, will have sharp peaks if a trial frequency coincides with the frequency of the model (2.1). For this reason, the function $P(\omega)$ may be used as an estimator of the power spectrum. Following Lomb (1976), we call this estimator the LS-spectrum. Its final representation is

$$P(\omega) = \frac{1}{2}\sum_{i=1}^{2} a_i(x,\phi_i). \tag{2.14}$$

The factor $\frac{1}{2}$ is introduced for convenience of comparison befween the LS-spectrum and the Schuster periodogram.

3 THE TYPES OF THE LS-SPECTRA

It is a common practice to use the term "periodogram" to designate an estimator of the power spectrum. In this sense, the various types of the LS-spectra considered in this paper will be called periodograms with the names of their authors.

3.1 The Barning Periodogram

Although the numerical least-squares algorithm was widely used to obtain the values of the a_1 and a_2 in spectral analysis of time series, it was Barning (1962) who first introduced the concept of the LS-spectrum and derived its analytical representation. In our notation, the expression for the Barning periodogram follows from Eqs. (2.8) and (2.14) in the form:

$$B(\omega) = \frac{1}{2}\frac{||\phi_1||^2(x,\phi_2) + ||\phi||^2||(x,\phi_1)^2 - 2(\phi_1,\phi_2)(x,\phi_1)(x,\phi_2)}{||\phi_1||^2||\phi_2||^2 - (\phi_1,\phi_2)^2}. \quad (3.1)$$

3.2 The Lomb Periodogram

To study the statistical properties of the LS-spectrum, it is desirable to have it as a sum of two squared functions. This can be done by several methods. One of them was proposed by Lomb (1976). His approach is based on the introduction of the new time points

$$\bar{t}_k = t_k - \tau(\omega), \quad (3.2)$$

where the time shift

$$\tau(\omega) = \frac{1}{2\omega}\arctan\frac{\Sigma_k \sin 2\omega t_k}{\Sigma_k \cos 2\omega t_k} \quad (3.3)$$

provides the orthogonality of the functions

$$\bar{\phi}_1(t) = \cos\omega\bar{t}_k, \quad (3.4)$$

$$\bar{\phi}_2(t) = \sin\omega\bar{t}_k. \quad (3.5)$$

Under this assumption the Lomb periodogram looks as follows:

$$L(\omega) = \frac{1}{2}\left[\frac{(x,\bar{\phi}_1)^2}{||\bar{\phi}_1||^2} + \frac{(x,\bar{\phi}_2)^2}{||\bar{\phi}||^2}\right]. \quad (3.6)$$

Following this idea, Scargle (1982, 1989) introduced a specific kind of the discrete Fourier transform:

$$FT(\omega) = \frac{1}{\sqrt{2}}\exp(-i\omega t_0)\left(x, \frac{\bar{\phi}_1}{||\bar{\phi}_1||} + i\frac{\bar{\phi}_2}{||\bar{\phi}_2||}\right), \quad (3.7)$$

in terms of which the Lomb periodogram becomes

$$L(\omega) = |FT(\omega)|^2. \quad (3.8)$$

3.3 The Ferraz–Mello Periodogram

Another method to express the periodogram as a sum of two squared quantities was proposed by Ferraz–Mello (1981). His approach is based on representing the data by orthogonal functions ψ_0 , ψ_1, ψ_2 which can be derived from the initial functions 1, ϕ_1, ϕ_2 by means of the Gram–Schmidt procedure. Obviously, this method corresponds to a "sinusoid plus constant" model. To simplify discussion and to make the results comparable to the "sinusoid" model which is the cornerstone in the Barning's and the Lomb's techniques, we shall apply the orthogonalization procedure to our functions ϕ_1, ϕ_2. The corresponding orthogonalized functions are:

$$\psi_1 = \phi_1, \tag{3.9}$$

$$\psi_2 = \phi_2 - \frac{(\phi_1, \phi_2)}{||\phi_1||}\phi_1, \tag{3.10}$$

$$||\psi_1||^2 = ||\phi_1||^2, \tag{3.11}$$

$$||\psi_2||^2 = ||\phi_2 - \frac{(\phi_1, \phi_2)^2}{||\phi_1||^2}. \tag{3.12}$$

The final expression for the Ferraz–Mello periodogram looks as follows:

$$FM(\omega) = \frac{1}{2}\left[\frac{(x, \psi_1)^2}{||\psi_1||^2} + \frac{(x, \psi_2)^2}{||\psi_2||^2}\right] \tag{3.13}$$

or

$$FM(\omega) = \frac{1}{2}|DCDFT(\omega)|^2, \tag{3.14}$$

where

$$DCDFT(\omega) = \left(x, \frac{\psi_1}{||\psi_1||} + i\frac{\psi_2}{||\psi_2||}\right) \tag{3.15}$$

is a new type of transform (the Date-Compensated Discrete Fourier Transform).

4 THE SCHUSTER PERIODOGRAM

In our notation, this "classical" estimator of the power spectrum can be written in the form

$$S(\omega) = (x, \phi_1)^2 + (x, \phi_2)^2 = \frac{1}{N^2}|\sum_{k=0}^{N-1} x_k e^{-i\omega t_k}|^2. \tag{4.1}$$

This expression shows that if the signal contains a sine function of frequency ω_0, then the product $x_k e^{-i\omega t_k}$ makes a large contribution to S provided that $\omega = \omega_0$. In other words, the Schuster periodogram, to the limit of normalizing factor, is a square of the correlation coefficient between the data and a harmonic function. Thus we see that the Schuster periodogram differs from the LS-spectra by definition. It is likely that due to the correlation nature, the Schuster periodogram and the true power spectrum $G(\omega)$ of the function

$$x(t) = A\cos(\omega_0 t + \phi_0) \tag{4.2}$$

are connected by the next relation (Vityazev, 1994):

$$S(\omega) = \int_{-\infty}^{+\infty} G(\omega)W(\omega - \omega')\, d\omega' + S_0(\omega), \tag{4.3}$$

where

$$4S_0(\omega) = A^2[\Omega(\omega-\omega_0)\Omega^*(\omega+\omega_0)e^{i2\phi_0} + \Omega^*(\omega-\omega_0)\Omega(\omega+\omega_0)e^{-i2\phi_0}], \tag{4.4}$$

$$\Omega(\omega) = \frac{1}{N}\sum_{k=0}^{N-1} e^{-i\omega t_k}, \tag{4.5}$$

$$W(\omega) = |\Omega(\omega)|^2. \tag{4.6}$$

Henceforth, the functions $\Omega(\omega)$ and $W(\omega)$ will be referred to *as the complex spectral window* and *the spectral window*, respectively. A set of functions given by Eq. (4.2), with phases ϕ_0, randomly distributed within the interval $[0, 2\pi]$, may be regarded as a stationary stochastic process. Averaging Eq. (4.4) over the set of realizations yields $\langle S_0 \rangle = 0$, thus reducing Eq. (4.2) to a convolution of the true spectrum $G(\omega)$ with the spectral window $W(\omega)$. This result was obtained by Deeming (1975), who studied the Schuster periodogram averaged over the realizations, given at the same set of arbitrary time points. It is very important to emphasize that the transition from $G(\omega)$ to $S(\omega)$ is completely explained by the spectral window $W(\omega)$. In particular, the convolution term in Eq. (4.3) reveals all the artifacts introduced into the periodogram by missing points (Deeming, 1975; Vityazev, 1994). Thus we see that the spectral windows, depending only on the distribution of time points, are very useful tools in spectral analysis, and we shall use them intensively in the next sections.

5 THE SCHUSTER PERIODOGRAM AND THE LS-SPECTRA

In this section we compare our periodograms. At first, the intercomparison between the LS-spectra is made.

Theorem 1. For any time series given at arbitrary time points, the Ferraz–Mello periodogram and the Barning periodogram are identical.

To prove this theorem, we write the obvious relations that can be obtained from Eqs. (3.9)–(3.12):

$$(x, \psi_1) = (x, \phi_1), \tag{5.1}$$

$$(x, \psi_2) = (x, \phi_2) - \frac{(\phi_1, \phi_2)}{||\phi_1||^2}(x, \phi_1), \tag{5.2}$$

$$||\psi_1||^2||\psi_2||^2 = ||\phi_1||^2||\phi_2||^2 - (\phi_1, \phi_2)^2. \tag{5.3}$$

Now, the identity $FM(\omega) = B(\omega)$ follows from Eq. (3.13), if Eqs. (5.1)–(5.3) are taken into consideration.

Theorem 2. For any time series given at arbitrary time points, the Lomb periodogram and the Barning periodogram are identical.

To prove this theorem, we shall use the relations:

$$(x, \bar{\phi}_1) = C_\tau(x, \phi_1) + S_\tau(x, \phi_2), \tag{5.4}$$

$$(x, \bar{\phi}_2) = C_\tau(x, \phi_2) - S_\tau(x, \phi_1), \tag{5.5}$$

where

$$C_\tau = \cos \omega\tau, \quad S_\tau = \sin \omega\tau. \tag{5.6}$$

It is not difficult to show that

$$2||\bar{\phi}_1||^2 = 1 + \sqrt{W(2\omega)}, \tag{5.7}$$

$$2||\bar{\phi}_2||^2 = 1 - \sqrt{W(2\omega)}; \tag{5.8}$$

$$\cos 2\omega\tau = \frac{Re\Omega(2\omega)}{\sqrt{W(2\omega)}}, \tag{5.9}$$

$$\sin 2\omega\tau = \frac{Im\Omega(2\omega)}{\sqrt{W(2\omega)}}. \tag{5.10}$$

Substitution of Eqs. (5.5)–(5.10) into Eq. (3.6) gives the identity $L(\omega) = B(\omega)$ if the relation

$$||\bar{\phi}_1||^2||\bar{\phi}_2||^2 = ||\phi_1||^2||\phi_2||^2 - (\phi_1, \phi_2)^2 = 1 - W(2\omega) \tag{5.11}$$

is taken into account.

Now we see that different expressions which define the Barning, the Lomb, and the Ferraz–Mello periodograms give one and the same result, and thus the general name for them – the LS-spectrum – is justified.

In order to compare the Schuster periodogram with the LS-spectrum, we rewrite Eq. (3.1) in the form:

$$B(\omega) = \frac{a^2(\omega)(x, \phi_1)^2 + b^2(\omega)(x, \phi_2)^2 - r(x, \phi_1)(x, \phi_2)}{1 - r^2}, \tag{5.12}$$

where

$$a^{-2} = 2||\phi_1||^2 = 1 + Re\Omega(2\omega), \tag{5.13}$$

$$b^{-2} = 2||\phi_2||^2 = 1 - Re\Omega(2\omega), \tag{5.14}$$

$$r = \frac{(\phi_1, \phi_2)}{||\phi_1|| \, ||\phi_2||} = \frac{Im\Omega(2\omega)}{\sqrt{1 - Re^2\Omega(2\omega)}}. \tag{5.15}$$

Suppose that

$$Im\Omega(2\omega) = \frac{1}{N}\sum_{k=0}^{N-1} \sin(2\omega t_k) = \frac{1}{2}(\phi_1, \phi_2) = 0, \tag{5.16}$$

$$Re\Omega(2\omega) = 0, \tag{5.17}$$

and, consequently,

$$W(2\omega) = 0. \tag{5.18}$$

In this case, the right-hand sides of Eqs. (4.1) and (5.12) coincide, and we come to the main conclusion of the present paper:

Theorem 3. *At the set of frequencies that satisfy Eq. (5.18), the Schuster periodogram and the LS-spectra are identical, otherwise they differ, and the closer to zero is the value* $1 - W(2\omega)$, *the stronger is their difference.*

Thus we see that the degree of likeness between the Schuster periodogram and the LS-spectra depends on the structure of the spectral window. In the next section we shall demonstrate several important distributions of time points for which the frequencies that satisfy Eq. (5.18) do exist.

6 THE SPECTRAL WINDOWS FOR TYPICAL DISTRIBUTIONS OF TIME POINTS

As we have seen, the key problem in the intercomparison between the spectra estimators is the study of the spectral windows. For any set of time points, the numerical calculation of the spectral windows can be done without problems. In this section we consider some typical distributions of points for which the spectral windows have analytical representations.

6.1 The Regular Time Series

In this case the sequence of time points is

$$t_k = \Delta t k, \; k = 0, 1, \ldots, N-1, \tag{6.1}$$

where Δt is a constant interval. For simplicity we consider N as an even number. The analytical forms of the spectral windows are known to be

$$W(\omega) \equiv W_0(\omega, N, \Delta t) = \frac{\sin^2(N\omega\Delta t/2)}{N^2 \sin^2(\omega\Delta t/2)}, \tag{6.2}$$

$$Re\Omega(\omega) = \frac{\sin(N\omega\Delta t/2)}{N \sin(\omega\Delta t/2)} \cos((N-1)\omega\Delta t/2), \tag{6.3}$$

$$Im\Omega(\omega) = \frac{\sin(N\omega\Delta t/2)}{N \sin(\omega\Delta t/2)} \sin((N-1)\omega\Delta t/2). \tag{6.4}$$

Usually, the Schuster periodogram is evaluated at the set of natural frequencies

$$\omega_j = \frac{2\pi}{N\Delta t} j, \; j = 0, 1, \ldots, \frac{N}{2} - 1. \tag{6.5}$$

It is easy to verify that

$$W(2\omega_j) = 0. \tag{6.6}$$

This gives us the first real example of a time points distribution, when the frequencies that satisfy Eq. (5.18) do exist. Now, we can conclude: in the case of regular observations the Schuster periodogram and the LS-spectra are identical provided their values are calculated at the natural frequencies (6.5).

6.2 Time Series with Periodic Gaps

The astronomical observations are often performed with periodic or quasi-periodic gaps. Ground-based observations are interrupted by day-night alteration giving gaps with the 24-hour period; the meteorological changes for a given site are repeated annually; the observations from a space vehicle are usually stopped when the satellite enters the radiation belts. To make a model of time points distributed with periodical gaps, we suppose that, in the set of regular observations with a constant sampling interval Δt, one has n succesive observations and p succesive missing points, and the group of $n+p$ points is repeated m times. In this case the period of gaps is $\Delta T = (n+p)\Delta t$. In the previous papers (Vityazev, 1994; Vityazev and Prudnikiva, 1994) we have shown that in this case the spectral window looks as follows:

$$W(\omega) = W_0(n, \omega, \Delta t) W_0(m, \omega, \Delta T), \tag{6.7}$$

where W_0 is given by Eq. (6.2). Due to gaps in observations, the spectral window $W(\omega)$ has well-pronounced *side peaks* at the *proper frequencies*

$$\bar{\omega}_l = \frac{2\pi}{m(n+p)\Delta t} l, \; l = 1, 2, \ldots, (n+p)/2. \tag{6.8}$$

If in our set of $m(n+p)$ points all the missing points all are filled in, then we can introduce the set of natural frequencies

$$\omega_j = \frac{2\pi}{m(n+p)\Delta t} j, \; j = 1, 2, \ldots, m(n+p)/2. \tag{6.9}$$

Excluding from ω_j the values $\bar{\omega}_l/2$, we form a new set of frequencies:

$$\omega_j^* = \frac{2\pi}{m(n+p)\Delta t} j, \; j = 1, 2, \ldots, m/2-1, m/2+1, \ldots m-1, m+1, \ldots, m(n+p)/2-1, \tag{6.10}$$

which satisfy Eq. (5.18). This gives us reason to state that when the frequency of gaps is $\bar{\omega}_1 = 2\pi/T$, the Schuster periodogram and the LS-spectra calculated at the

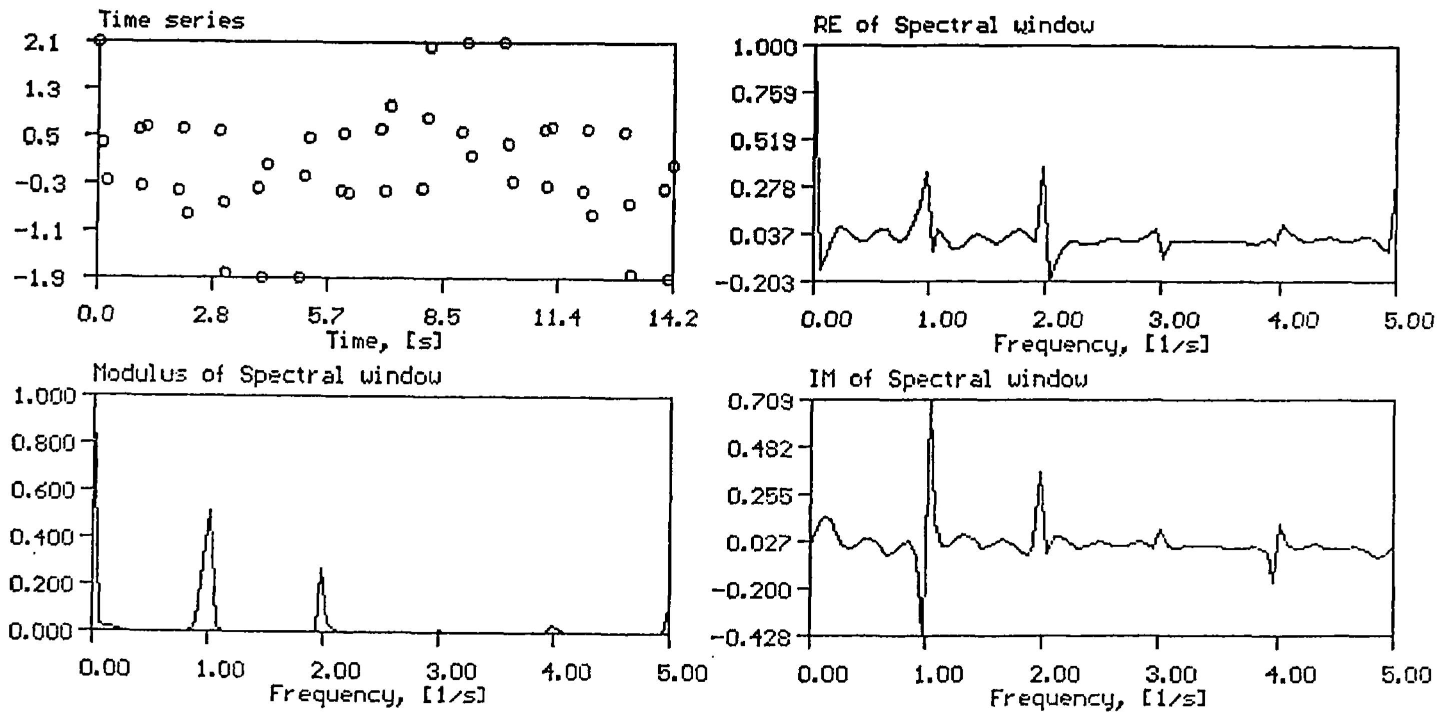

Figure 1 Functions $W(\omega)$, $Re\Omega(\omega)$, and $Im\Omega(\omega)$ for the set of time points with periodic gaps ($n = 3$; $p = 7$; $m = 15$).

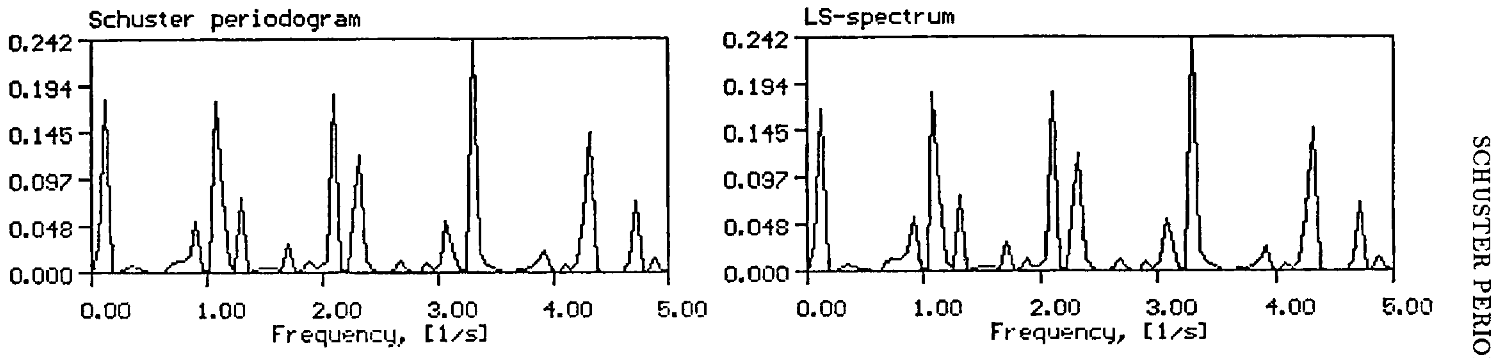

Figure 2 Coincidence of the Schuster periodogram and the LS-spectra for the set of time points with periodic gaps.

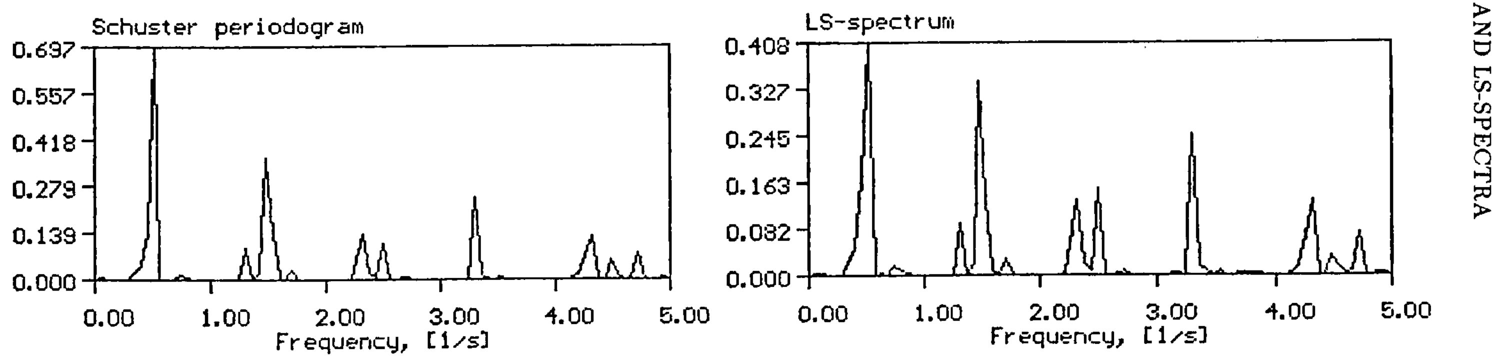

Figure 3 Deviation of the Schuster periodogram from the LS-spectra for the set of time points with periodic gaps.

frequencies ω_j^* are the same, provided that the frequencies of the harmonics in the data do not coincide with the values $\bar{\omega}_l/2$. Figure 1 shows the time series

$$x(t) = A_1\cos(2\pi\nu_1 t) + A_2\cos(2\pi\nu_2 t), \qquad (6.11)$$

generated at the time points with periodical gaps ($n = 3, p = 7, m = 15, \Delta t = 0.1s$), and the functions $W(\omega)$, $Re\Omega(\omega)$, and $Im\Omega(\omega)$, corresponding to this distribution of time points. We see that the side peaks are located at the proper frequencies $\nu_1 = 1, \nu_2, \ldots, \nu_5 = 5$. In Figure 2 we show the Schuster periodogram and the LS-spectrum, calculated for the parameters $A_1 = 1$, $A_2 = 1$, $\nu_1 = 1.1$ Hz, $\nu_2 = 3.3$ Hz. We see, that all the periodograms are identical, since no one of the values $2\nu_1$ and $2\nu_2$ coincides with the proper frequencies $\bar{\nu}_j$, at which $W(\bar{\nu}_j) \neq 0$. The opposite case is shown in Figure 3, where our periodograms were calculated for $A_1 = 1$, $A_2 = 1$, $\nu_1 = 0.5$ Hz, $\nu_2 = 3.3$ Hz. Now we have $2\nu_1 = \bar{\nu}_1 = 1$ Hz, that is why the Schuster periodogram drastically differs from the *LS*-spectrum.

6.3 Observations with a Long Gap

Considered here is a situation when two sets of observations (each one consisting of n successive points) are separated by p missing points forming the gap. As earlier, all the points are supposed to be regularly spaced over the time interval $\Delta t =$ const. Now, for the spectral window we have (Vityazev, 1994):

$$W(\omega) = W_0(n, \omega, \Delta t)[\cos((n+p)\omega\Delta t)]/2. \qquad (6.12)$$

It is not difficult to show that the frequencies

$$\omega_j^* = \frac{\pi}{(n+p)\Delta t}(j + \frac{1}{2}),\ j = 0, 1, \ldots, n+p-1, \qquad (6.13)$$

satisfy the condition (6.6). It is important to note that the proper frequencies of the spectral window (6.12) defined as

$$\bar{\omega}_k = \frac{2\pi}{(n+p)\Delta t}k,\ k = 1, 2, \ldots, \qquad (6.14)$$

do not coinside with the values $2\omega_j^*$. In Figure 4 the functions $W(\omega)$, $Re\Omega(\omega)$ and $Im\Omega(\omega)$ are shown for the distribution of time points with a gap ($n = 40$, $p = 40$, $\Delta t = 0.1s$). We see that all strong side peaks are concentrated in the low frequency region of the spectrum. Figure 5 demonstrates our periodograms for the function (6.11) with parameters $A_1 = 1$, $A_2 = 1$, $\nu_1 = 1.1$ Hz, $\nu_2 = 3.3$ Hz. All the periodograms turned out to be identical since the doubled frequenvies $2\pi\nu_1$ and $2\pi\nu_2$ have been taken not equal to the proper frequencies $\bar{\omega}_k$. On the contrary, the values $\nu_1 = 0.0625$ Hz and $\nu_2 = 3.3$ Hz yield quite different periodograms (Figure 6), since in this case we have $4\pi\nu_1 = \bar{\omega}_1$.

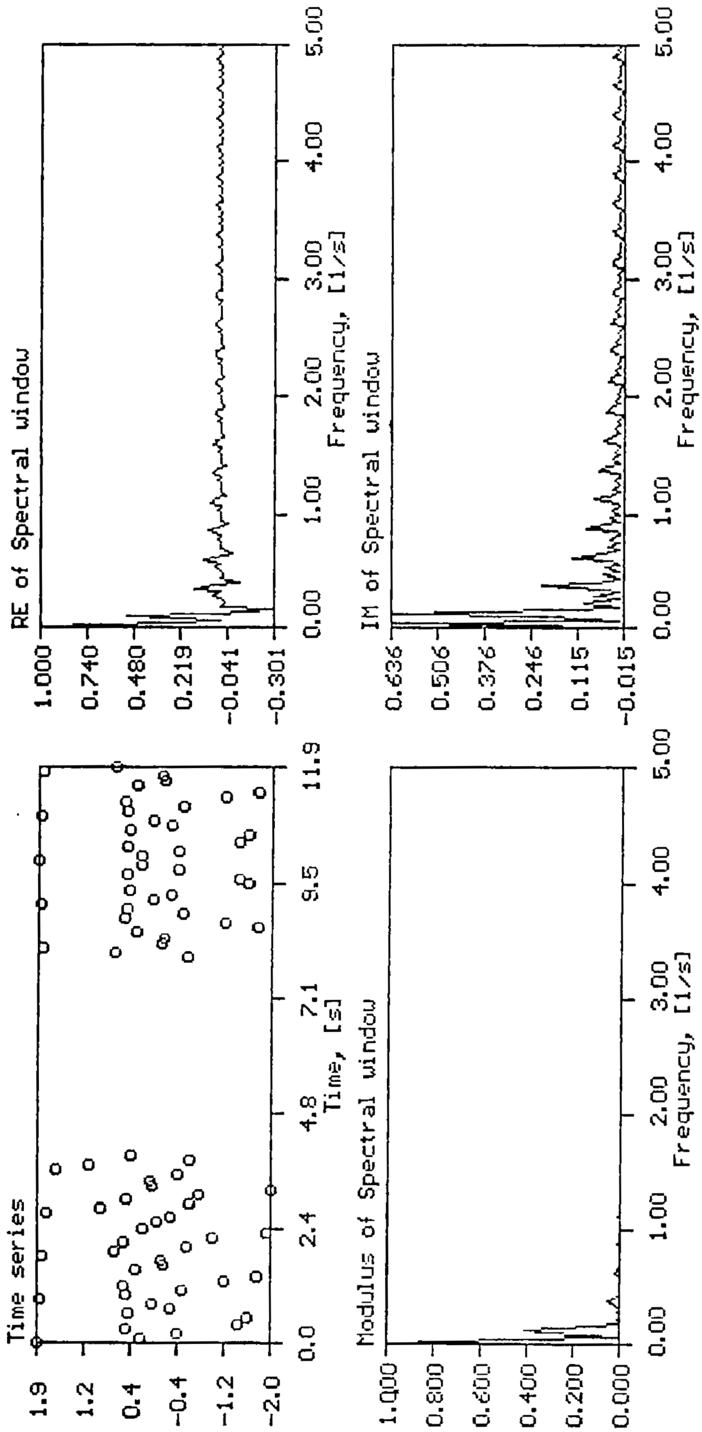

Figure 4 Functions $W(\omega)$, $Re\Omega(\omega)$, and $Im\Omega(\omega)$ for the set of time points with a long gap ($n = 40; 40$).

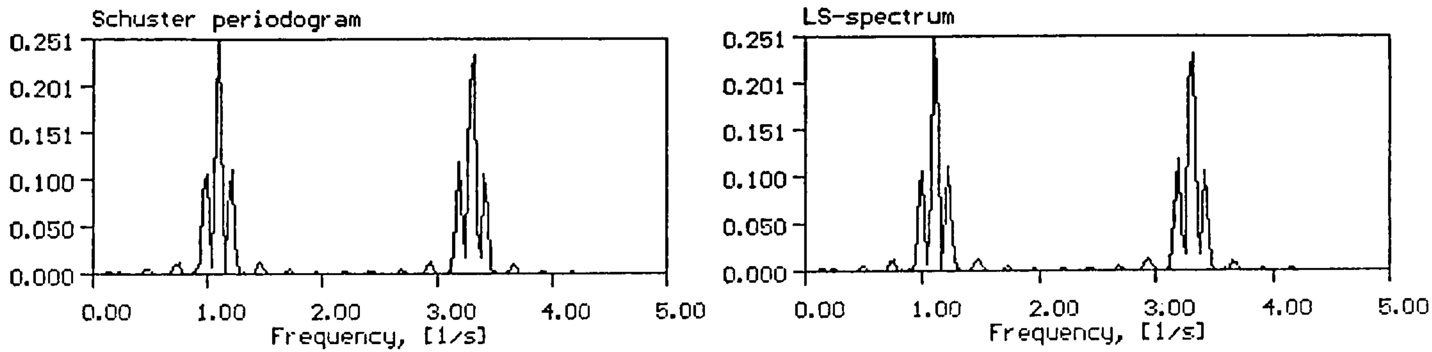

Figure 5 Coincidence of the Schuster periodogram and the LS-spectra for the set of time points with a long gap.

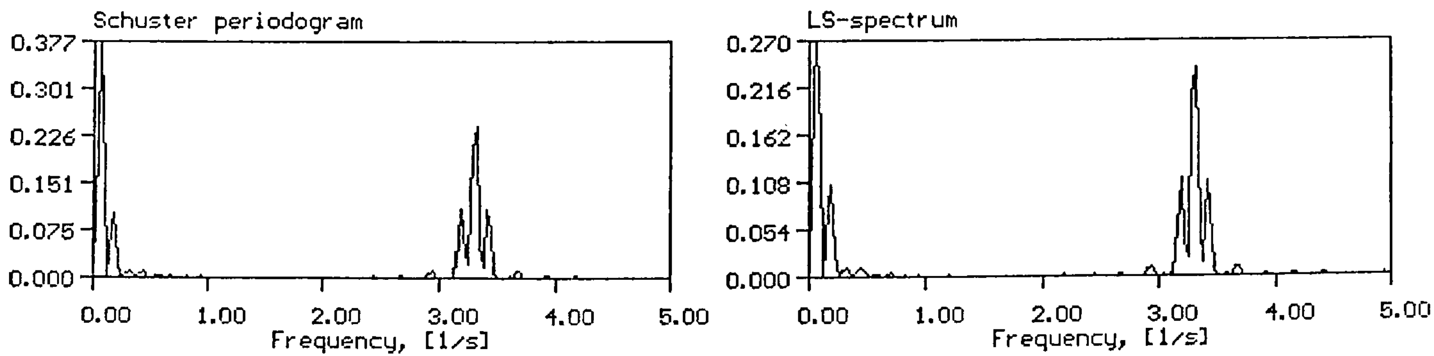

Figure 6 Deviation of the Schuster periodogram from the LS-spectra for the set of time points with a long gap.

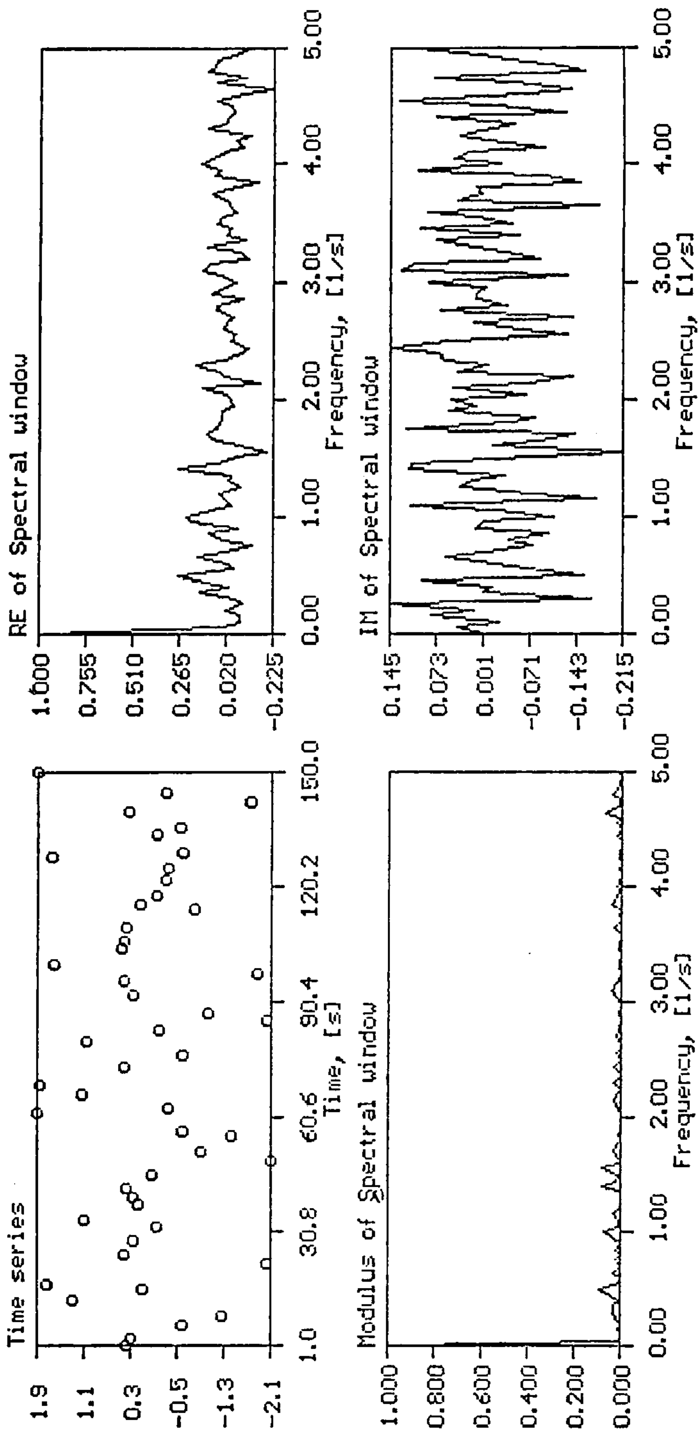

Figure 7 Functions $W(\omega)$, $Re\Omega(\omega)$, and $Im\Omega(\omega)$ for the set of 50 irregularly distributed time points.

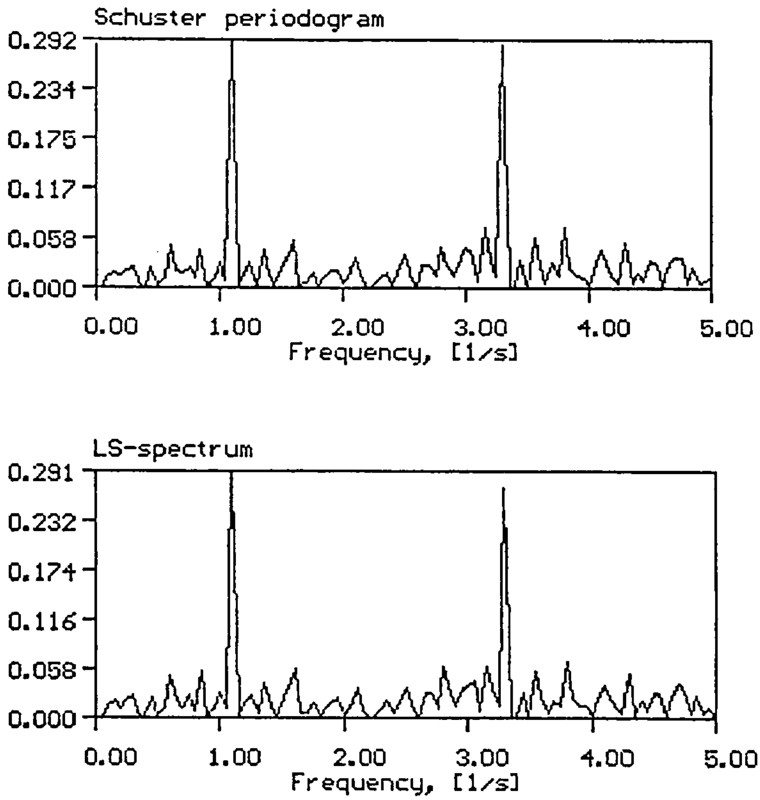

Figure 8 The Schuster periodogram and the LS-spectra for the set of 50 irregularly distributed time points.

6.4 Time Series with Random Distribution of Points

It is likely that no analytical expression for the spectral window exists in this situation. The numerical experiments give evidence that the spectral windows, despite the central peak at $\omega = 0$, have a number of side peaks irreqularly distributed in the frequency domain. These peaks have no tendency to be concentrated at some specific frequencies and, as a rule, the intencities of the side peaks are small if compared to the central peak.

Figure 7 shows the functions $W(\omega)$, $Re\Omega(\omega)$ and $Im\Omega(\omega)$ for the set of 50 time points which randomly deviate from the even grid of points. We see the irregularities specific to the case, but since there are no frequencies at which the values of the spectral window are large, we can hope that the Schuster periodogram and the LS-spectrum will not differ considerably. This is confirmed by Figure 8, where our periodograms calculated for the function (6.11) with parameters $A_1 = 1$, $A_2 = 1$, $\nu_1 = 1.1$ Hz, $\nu_2 = 3.3$ Hz are shown.

7 MIXTURE OF PERIODICITIES

As we have seen, at the frequencies defined by Eq. (5.18) all the periodograms under consideration are identical. In this section the opposite case is studied, that is, we try to answer the question: what happens when we have the condition

$$1 - W(2\omega) \ll 1. \tag{7.1}$$

First of all, let us write the expressions which show the intensity of the peak centered at ω_0, where ω_0 is the frequency of a sine function given by Eq. (4.2). For the Schuster periodogram, from Eqs. (4.3) and (4.4) we have:

$$S(\omega_0) = \frac{A^2}{4}[1 + W(2\omega_0)] + \frac{A^2}{2} Re\Omega(2\omega_0) \cos 2\phi_0 - \frac{A^2}{2} Im\Omega(2\omega_0) \sin 2\phi_0, \tag{7.2}$$

where ϕ_0 is the phase of the sine fuction. The analogous equation valid for the LS-spectrum looks as follows:

$$B(\omega_0) = \frac{A^2}{4}[1 + Re\Omega(2\omega_0) \cos 2\phi_0 - Im\Omega(2\omega_0) \sin 2\phi_0]. \tag{7.3}$$

In Table 1 we show the intensities of the peak centered at frequency $\nu_0 = 0.5$ Hz in the Schuster periodogram and in the LS-spectra for the sine function (4.2) with parameters $A = 1$, $\omega_0 = 2\pi\nu_0$ with different values of the phase. The sine function (4.2) was calculated at the set of time points with periodical gaps ($n = 3$, $p = 7$, $m = 20$, $\Delta t = 0.1s$). In this case, $W(2\omega_0) = 0.762$; $Re\Omega(2\omega_0) = 0.706$; $Im\Omega(2\omega_0) = 0.513$, so the condition (7.1) is satisfied. Two striking conclusions follows from Table 1: a) the dependence on phase is strong for all the periodograms; b) no one of them gives the expected value $A^2/4 = 0.25$. Thus we see that in the specific case defined by (7.1) all our periodograms are bad. This gives reason to suspect that in this situation ***something happens with the time series itself.***

To study this, let us represent the observed time series as follows:

$$y(t) = w(t)x(t), \tag{7.4}$$

where $x(t)$ denotes the polyharmonical function given for $|t| < \infty$, and $w(t)$ is the time window defined as unity for $t = t_k$ and as zero elsewhere. For the time series

Table 1.

$\phi°$	S	LS
0	0.793	0.426
45	0.184	0.122
90	0.087	0.074
135	0.697	0.378
180	0.793	0.426

with periodic gaps, considered in Subsection 6.2, the time window can be replaced by its Fourier series:

$$w(t) = \alpha_0 + \sum_{l=1}^{\infty} \gamma_l \cos(\bar{\omega}_l t + \phi_l), \tag{7.5}$$

where $\bar{\omega}_l$ are the proper frequencies defined by (6.8). If the function $x(t)$ is given by Eq. (4.2), then we have:

$$\begin{aligned} y(t) &= \alpha_0 A \cos(\omega_0 t + \phi_0) \\ &+ \frac{A}{2}\sum_{l=1}^{\infty} \gamma_l \cos[(\bar{\omega}_l + \omega_0)t + \phi_l + \phi_0] \\ &+ \frac{A}{2}\sum_{l=1}^{\infty} \gamma_l \cos[(\bar{\omega}_l - \omega_0)t + \phi_l - \phi_0]. \end{aligned} \tag{7.6}$$

The power spectrum of this function consists of lines (of peaks, when the periodogram analysis is used) at the frequencies $\pm\omega_0$ that correspond to the signal and lines at $|\bar{\omega}_l \pm \omega_0|$ which are usually called "the ghosts", i.e. false lines due to gaps in observations. In the case of periodic gaps, the ghosts follow each other with the unterval $\Delta\omega = \bar{\omega}_1 = 2\pi/\Delta T$. If $2\omega_0 \neq \bar{\omega}_1$, then the ghosts of the true lines located at $\pm\omega_0$ do not interfere. Otherwise, they coincide and change the intensities of the lines. This is clearly seen in the time domain too, for if we put $\omega_0 = \bar{\omega}_1/2$, then Eq. (7.6) yields

$$\begin{aligned} y(t) &= \alpha_0 A \sqrt{1 + \beta_1^2 + 2\beta_1 \cos(2\phi_0 - \phi_1)} \cos(\omega_0 t + \psi) \\ &+ \frac{A}{2}\sum_{l=1}^{\infty} \gamma_l \cos[(\bar{\omega}_l + \omega_0)t + \phi_l + \phi_0] \\ &+ \frac{A}{2}\sum_{l=2}^{\infty} \gamma_l \cos[(\bar{\omega}_l - \omega_0)t + \phi_l - \phi_0], \end{aligned} \tag{7.7}$$

where

$$\tan\psi = \tan\phi_0 \frac{1 + \beta_1 \frac{\sin(\phi_1 - \phi_0)}{\sin\phi_0}}{1 + \beta_1 \frac{\cos(\phi_1 - \phi_0)}{\cos\phi_0}}, \tag{7.8}$$

$$\beta_1 = \gamma_1 / 2\alpha_0. \tag{7.9}$$

Comparison between Eqs. (4.2) and (7.7) shows that the observations with periodic gaps change the amplitude and the phase of the initial signal. It is true that, due to the rectangular form of the function $w(t)$, the Fourier series (7.5) converges to $\frac{1}{2}$ (not to 1) at the first and the nth points in each segment of $n + p$ points. For this reason, Eqs. 7.4 and 7.6 coincide everywhere except these points. Nevertheless, this defect of convergence does not play a crucial role in our analysis, and our main conclusion is: if *a harmonic process of frequency* ω_0 *is observed with periodic gaps of frequency* $2\omega_0$*, then the observed time series becomes a mixture of these two periodic* *processes.* We would obtain the same results each time when the condition (7.1) is satisfied. In such pathological situations, the estimation of the power spectrum will be wrong, *no matter what estimator (from those considered in this paper) is used.*

8 CONCLUSIONS

The results of this study may be summarized as follows:
a) all the LS-spectra considered in this paper – the Barning, the Lomb, and the Ferraz–Mello periodograms (based on the pure sinusoid model) – are identical;
b) the likeness between the Schuster periodogram and the LS-spectra is governed by the behavior of the spectral window;
c) at those frequencies where $W(2\omega) = 0$, all the periodograms under consideration are identical.
d) if the maxima of the spectral window (except the central peak) are small, then all the periodograms are nearly identical;
e) the Schuster periodogram differs from the LS-spectra only at the frequencies that satisfy the condition $1 - W(2\omega) \ll 1$. It means that the discrepancies between the Schuster periodogram and the LS-spectra are large when the time series contain a harmonic of the frequency, the double value of which coincides with the frequency at which the spectral window has a large side peak. In the case of periodical gaps, it happens when the period of a signal hidden in the data is one half the period of the gaps. In this pathological situation, the spectral estimation faces unrealistic intensities of the spectral peaks and the strong dependence of the hights of peaks on the phase of the signal. It is very important to emphasize that these problems come not from the choise of the periodogram-the problems are hard for all the periodgrams that we have studied-but they originate from mixing two sources of the periodicities: one is the physical process that we observe and another one is a periodical interruption of observations. In astronomy, the rotation and revolution of the Earth impose diurnal and annual cycles on the Earth-based observations. The periods hidden in observations of the Sun, stars, quasars, etc., are hardly connected physically with the periods specific to the Earth. For these observations, the probability to come across the mixing of the periodicities is negligible. On the contrary, if we study the Earth from the Earth (such is the case with the astrometric observations of the Earth's rotation parameters), then the semi-annual period known in the Earth rotation interferes with the annual gaps in observations.

Nevertheless, exept for pathological situations, the Schuster periodogram is practically identical to the LS-spectra. This forces us to to make a closer examination of the statistical properties of the Schuster periodogram for uneven time series. And this is a topic for the next article.

References

Barning, F. J. M., (1962) *B.A.N.* **17**, No. 1, 22.
Deeming, T. J. (1975a) *Astrophys. Space Sci.* **36**, 137.

Deeming, T. J. (1975b) *Astrophys. Space Sci.* **42**, 257(E).
Ferraz-Mello, S. (1981) *Astron. J.* **86**, 619.
Jenkins, G. M. and Watts, D. G. (1968) *Spectral analysis and its applications*, Holden–Day, San Francisco.
Lomb, N. R. (1976) *Astrophys. Space Sci.* **39**, 447.
Marple, Jr., S. L. (1987) *Digital Spectral Analysis with Applications*, Prentice-Hall, Englewood Cliffs, New Jersey.
Otnes, R. K. and Enocson, L. (1978) *Applied Time Series Analysis*, A Wiley–Interscience Publication, New York.
Roberts, D. H., Lehar, J., and Dreher, J. W. (1987) *Astron. J.* **93**, 968.
Scargle, J. D. (1982) *Astrophys. J.* **263**, 835.
Scargle, J. D. (1989) *Astrophys. J.* **343**, 874.
Schuster, A. (1898) *Terrestrial Magnetism* **3**, 13.
Terebish V. Yu. (1992) *Time Series Analysis in Astrophysics*, Moscow, Nauka.
Vityasev, V. V. (1994) *Astron. and Astrophys. Tr.* **5**, 177.
Vityasev, V. V. and Prudnikova, E. Ya. (1994) *Vestn. St. Petersburg Univ.*, Ser. 1, issue 2, No. 8, 78.